Available online at www.sciencedirect.com
ScienceDirect
Physica A 371 (2006) 703–718
PHYSICA A
www.elsevier.com/locate/physa

# Multifractal character of surface latent heat flux

Nikitas Papasimakis[a], Guido Cervone[b], Fotini Pallikari[a,*], Menas Kafatos[b]

[a]Solid State Physics Department, School of Physics, University of Athens, Panepistimiopolis, Zografou 15784, Athens, Greece
[b]Center for Earth Observing and Space Research, George Mason University, Fairfax, VA 22030, USA

Received 11 November 2005; received in revised form 23 February 2006
Available online 2 May 2006

**Abstract**

Surface latent heat flux (SLHF) has been associated with the study of natural hazards, such as earthquakes and hurricanes and has been proposed as a useful quantity in the prediction and monitoring of their evolution. In the present study the Mediterranean Sea, parts of Europe, Africa and Turkey are mapped with regard to the multifractal characteristics of SLHF time series during a period of eight years (1997–2004). The estimated Hurst exponents are markedly larger over land than over sea. In the case of land, SLHF has the characteristics of a mean-averting process, while its records are over sea noticeably uncorrelated. In contrast to the rather monofractal and weak multifractal character observed in most regions, with the application of a detrended fluctuation analysis, intense multifractality is seen mainly in North Africa. Crossover segments are present in the scaling of negative moments, implying that the small SLHF fluctuations are affected by seasonal components. Identification of anomalous SLHF deviations from their long-term multifractal behavior may serve as a precursor of extreme atmospheric phenomena.


*Keywords:* Surface latent heat flux; Multifractal analysis; MF-DFA; Earthquake; Hurricane

## 1. Introduction

In the last decades significant advances have been made in our understanding of the interactions between the atmospheric and geophysical processes, mainly due to the use of very large databases obtained either from earth or remote satellite sensors. It has been proposed that atmospheric phenomena may prove useful in short-term earthquake prediction [1]. Surface latent heat flux (SLHF) is a geophysical parameter whose study has recently been related to earthquakes [2–4] and other natural hazards, such as cyclones and hurricanes. SLHF is associated with the phase change of water, and is directly proportional to the amount of evaporation on the surface of land and sea. In order to provide robust identification methods of possible precursors based on SLHF, which are usually in the form of anomalies such as the presence of singularities in the experimental time series, the long-term behavior of SLHF should be understood. Although the precise method for utilizing SLHF for short-term predictions of geophysical and atmospheric hazards is not yet well established, the

*Corresponding author. Tel./fax: +30 1 727 6823.
*E-mail addresses:* npapasim@phys.uoa.gr (N. Papasimakis), gcervone@gmu.edu (G. Cervone), fpallik@phys.uoa.gr (F. Pallikari), mkafatos@gmu.edu (M. Kafatos).

0378-4371/$ - see front matter 
doi:10.1016/j.physa.2006.03.053

severity of such phenomena makes it worth of further study. Moreover, since SLHF is a key factor of the Earth's energy budget, exploring it further can provide useful information in other areas of research such as meteorology and hydrology. We characterize in this work the multifractal behavior of SLHF time series for the region of the world over the Mediterranean Sea, parts of Europe, Africa and Turkey and for the period of eight years (1997–2004).

Fractals have been introduced in order to quantify the self-similarity observed in nature, while at the same time to make possible the study of non-differentiable processes [5–7]. Given that this self-similar behavior has often a "local" character (either in space or time), the theory of fractals was generalized to multifractals [7,8], enabling the description of more complex phenomena with varying fractal properties. Examples of processes that have been thus treated are the energy dissipation in turbulence [9] and the price increments in finance [10]. In the field of geophysics and atmospheric physics, fractal and multifractal analyses have been extensively applied [11,12], since self-similarity is present in a wide variety of such phenomena, from the distribution of earthquake epicenters [13–15] and hypocenters [16] to climate change [17] and atmospheric turbulence [18,19]. In the same field of research, fractal and multifractal methods have been used both to characterize the long-term behavior of related signals and to indicate possible precursors in experimental time series of their records, yielding very promising results [20–27].

An introduction to the SLHF geophysical parameter in Section 2 gives also information regarding the dataset used. Section 3 offers a brief overview of the theory of fractal and multifractal processes, while the methodology implemented is described in Section 4. The results of this multifractal analysis are presented in Section 5 and their significance in relation to natural hazards is discussed in Section 6.

## 2. Surface latent heat flux & dataset

SLHF is a key component of the Earth's energy budget and hydrological cycle. It represents the amount of energy moving from the surface to the air due to evaporation (positive values) or from the air to the land due to condensation (negative values) [28]. In that sense, water vapor is indeed very dynamic. It is transported vertically through atmospheric circulation as well as latitudinally from the equatorial regions towards the poles. At the poles it is condensed as rain or snow releasing the heat energy stored within the water molecules [29]. SLHF is generally higher over the sea, than is over the land, because of the presence of larger amounts of water changing into water vapor.

SLHF records are the product of several parameters such as primarily surface air temperature, humidity and wind speed [30]. These parameters are recorded in situ with devices on buoys and ships, and even from large distances by remote sensing devices on satellites [31]. SLHF, as a derived observable, may be subjected to partial errors due to inaccuracies in the individual measurements, or even due to omission of other parameters that have been considered of lesser importance. Bentamy et al. [31] have discussed the different methods presently used to compute and validate various SLHF products.

SLHF plays an important role in the formation of hurricanes and cyclones, providing an early warning regarding their intensity and amount of rainfall once the storm makes landfall [32,33]. A hurricane begins to form when the latent heat is released as the clouds condense into liquid, warming the atmosphere. When the air becomes warmer, it expands producing an area of low pressure which becomes the center of the storm. Due to the low pressure gradient generated, warmer air moves towards the center of the forming hurricane from the surrounding areas, evaporating and causing this process to repeat and intensify. For the quantitative analysis of SLHF associated with severe atmospheric phenomena, like hurricanes and cyclones, it is worth understanding the evolution of SLHF time series and their multifractal characteristics due to its strong association with such phenomena.

A large-scale characterization of the multifractal properties of SLHF is not realizable and beyond the scope of this paper. We chose to analyze SLHF around the Mediterranean Sea where a variety of very different multifractal activities is observed. The SLHF data used for the present analysis consist of daily estimated values from 1/1/1997 to 31/12/2004, i.e., 2922 days, and cover a rectangular area over the Mediterranean of latitude from 29.52N to 50.48N and longitude from 5.62W to 41.25E, as shown in Fig. 1.

Although SLHF data are available from 1940, data prior to 1997 is found to be less reliable, and it was deliberately not included in this study. The data are estimated on a grid of equally spaced longitudinal lines

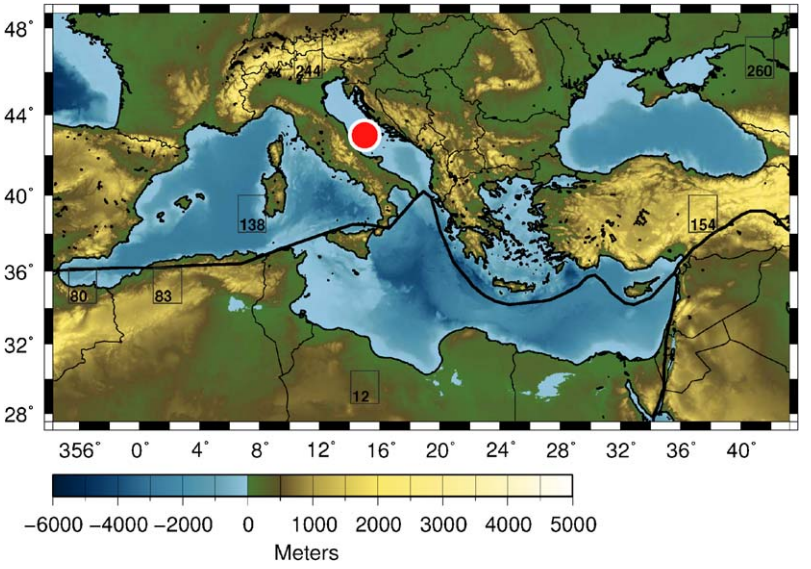


Fig. 1. Map of the area used in the analysis. Numbered squares: grids presenting characteristic behavior. Red circle: location where correlation between multifractal behavior and seismicity is observed.

with a 1.875° spacing and almost equally spaced latitudinal lines with an approximately 1.9° spacing. The SLHF records of the present dataset have been estimated from both in situ observations at various stations as well as from satellite data. Past observations are being reprocessed according to the NOAA NCEP/NCAR reanalysis project [34], in order to diminish the effect of frequent changes in assimilation methods. The data are available on line from the website of the Scientific Computing Division of the National Center for Atmospheric Research.[1]

## 3. Self-similar and multifractal processes

A process $Y_H(t)$, where $t>0$ is said to be self-similar with index $H$, if for every $\lambda>0$ the following relation with respect to the finite dimensional distributions (f.d.) holds [7]

$$Y_H(\lambda t) = \lambda^H Y_H(t). \tag{1}$$

The index $H$ is called the Hurst exponent[2] [35,36] and carries information in relation to the scaling of $Y_H(t)$ when the $t$-axis resolution is rescaled, i.e., when the process is observed over larger or smaller time lags. On the other hand, $H$ is a measure of the regularity of the process and consequently of the roughness of the graph of $Y_H(t)$ [6]. If $Y_H(t)$ has stationary increments, then $0<H<1$, while for differentiable processes or processes with non-stationary increments $H>1$. Totally uncorrelated processes with stationary increments exhibit $H=0.5$. For $H<0.5$ the process is mean-returning and is said to exhibit anti-persistent behavior, while for $H>0.5$ the process is mean-averting and persistent [36]. The graph of $Y_H(t)$ is then a fractal, with fractal dimension $D=2-H$ [6,37].

Scaling of the form of relation (1) is very restrictive in the case of real applications, since the singular behavior of natural processes often varies with time and a global Hurst exponent $H$ is not sufficient to characterize the process. In order to quantify the fractal characteristics of the process adequately in this instance, either a local time-dependent exponent $h(t)$ or the scaling of a distribution of generalized scaling exponents $h(q)$ is determined, where the parameter $q$ defines the order of the moment of this distribution (see Eq. (5)). In the first case, the local information of the process is preserved, which is lost in the second

[1] http://iridl.ldeo.columbia.edu/SOURCES/NOAA/NCEP-NCAR

[2] After the English hydrologist E. Hurst who observed self-similarity in the long-term behavior of the water influx of the Nile.

approach. However, since there is no robust method to estimate a local exponent from real data, the second procedure is usually followed. The process is then considered to be multifractal in both cases, in contrast to the monofractal processes described by relation (1).

In this context, the records of a process are considered to be measures over geometric supports (which in the case of time series analysis usually involves the time axis) exhibiting inhomogeneous scaling behavior. In fact, multifractal measures can be decomposed into interwoven fractal subsets, each one described by a different scaling exponent. However, in order to fully characterize multifractals, the "density" of occurrence of each fractal subset is also crucial. This information is provided by the multifractal (or singularity) spectrum function $f(h)$, which is related to the probability of observing a singularity of strength $h$ at any given scale. More precisely, while the exponent $h$ describes the scaling of the measure (or, of the process) in the "neighborhood" of a fixed point $t$, $f(h)$ defines the rate of exponential decay of the probability of observing $h$ in the "neighborhood"of any point in the time series. Furthermore, under certain conditions $f(h)$ can be considered as a box counting dimension of the set of points with exponent $h$ [9].

## 4. Methods

### 4.1. Normalization

A major issue in the fractal analysis of experimental time series is the detection and removal of periodic components. The presence of deterministic trends in time series has been studied thoroughly and it has been shown that it can bias the results of the analysis [38]. The procedure followed to minimize the presence of the strong periodical components in the SLHF records is the following. Each day of the year is taken to be the center of an 11-day window consisting of the five preceding days and the five days that follow. An average SLHF value is associated with each day in question being the mean of the corresponding 11 day window over all the years available, i.e., of the 11 days in 8 years, or 88 days. For the first and last five days of the year, the time series is padded periodically.[3] Finally, the SLHF record of each day is normalized by subtracting the corresponding to 88-day average.

### 4.2. MF-DFA analysis

The above normalization procedure may still leave SLHF time series at each location strongly non-stationary, as well as traits of seasonal components. That calls for the use of either the wavelet-based method [39] or the detrended fluctuation analysis (DFA) in order to eliminate any remaining trends, which could lead conventional methods to failure. In the current study of SLHF the multifractal DFA algorithm (MF-DFA) [40] has been selected for its high accuracy [41].

The MF-DFA proceeds as follows: let $Y(t)$ denote the time series where $t = 1, 2, \ldots, L$ and $L$ the length of the time series. First the profile $X(t)$ is defined as

$$X(t) = \sum_{j=1}^{t} (Y(j) - \langle Y \rangle), \tag{2}$$

where

$$\langle Y \rangle = \frac{1}{L} \sum_{j=1}^{L} Y(j) \tag{3}$$

is the mean of the time series. Then, a set of windows $N$ is selected such that $1 < N < L$, and the time series is divided in $[L/N]$ segments of size $N$, where $[L/N]$ denotes the integer part of $L/N$. Usually a very small number of data points, in comparison to $L$, remains after the $L/N$ division. In order to diminish the effect of deterministic trends in the estimation of the scaling exponents, we find the best (in a least-square sense) fitting polynomial $P(i, N)$ to $X(t)$ in each of the segments for each value of $N$, where $i = 1, 2, \ldots, [L/N]$. The

[3]For example, the 11-day window corresponding to the first day of January consists of 11 days from 26th December to 6th January.

detrended fluctuation $F$ is defined as the square root of the second order moment of the differences between the profile $X$ and the fitting polynomial $P$

$$F(i,N) = \sqrt{\frac{1}{N}\sum_{j=1}^{N}(X(j+(i-1)N) - P(i,N))^2}. \tag{4}$$

For future convenience we introduce the scale parameter $n = N/L$. Then, for each scale $n$, the $q$th root of the $q$th moment of the detrended fluctuation $F$ is considered:

$$Z(q,n) = \sqrt[q]{[n]\sum_{i=1}^{[1/n]} F(i,n)^q}, \tag{5}$$

where $q$ is a real parameter. The role of $q$ becomes obvious from the definition of $Z(q,n)$: for $q>0$ the largest fluctuations of $F$ will dominate the sum, while for $q<0$ the most important contribution to the sum comes from the smaller fluctuations of $F$. Finally, the scaling of $Z(q,n)$ with respect to the scale parameter $n$ is considered, i.e., the graph of $\log(Z(q,n))$ vs. $\log(n)$ is plotted for various values of $q$. For small enough $n$, it is expected that $Z(q,n)$ will scale as

$$Z(q,n) \propto n^{h(q)}, \tag{6}$$

where $h(q)$ is the generalized Hurst exponent. For $q = 2$, the $h(q = 2)$ provides the global Hurst exponent, $H$. If the series is monofractal then $h(q)$ is independent of $q$ and $h(q) = H$ for every $q$. In the case of multifractal series, $h(q)$ is usually continuous over the interval $[h_{min}, h_{max}]$ where $h_{min}, h_{max}$ are the minimum and maximum generalized Hurst exponents, respectively.

In our analysis the cut-off size of window, referring to the lowest parameter $N$ used, is fixed to 20 days in order to avoid the effect of the short-range correlations interfering with the normalization process. The upper limit is set to 500 days, since above that the sum of relation (5) contains very few terms (due to the finite length of the available time series) making the representation of the fluctuations inadequate. Finally, we consider only values $-1<q<5$ in order to provide satisfactory linear fits of $\log(Z(q,n))$ vs. $\log(n)$.

## 5. Results and discussion

Before discussing the results of the multifractal analysis of the SLHF time series, it is worth looking into its seasonal and geographical variation. Selected regions of interest are numbered by grid, Fig. 1 and Table 1. As expected, over the sea SLHF is higher than over land, Fig. 2.

The distinction between land and sea becomes less prominent in the winter, however. The regular seasonal pattern of SLHF reaches maximum during the warmer summer months around the southern parts of the Mediterranean Sea near Africa, primarily due to the warmer sea surface temperature, while maxima generally recorded over islands and coasts. SLHF reaches its minimum during the cooler winter months,

Table 1
Coordinates, global Hurst exponent ($H$) and range of generalized exponents ($R = h(q=-1) - h(q=+5)$) for small and large scales of the grids used

| Latitude | Longitude | Grid ID | $H$ | $R$ small (large) scales |
|---|---|---|---|---|
| 29.52N | 15E | 12 | 0.35 | 0.93 (0.93) |
| 35.24N | 3.75W | 80 | 0.52 | 1.43 (0.42) |
| 35.24N | 1.88E | 83 | 0.74 | 0.91 (0.91) |
| 39.05N | 7.5E | 138 | 0.49 | 0.27 (0.09) |
| 39.05N | 37.5E | 154 | 0.99 | 0.07 (–) |
| 46.67N | 11.25E | 244 | 1.03 | 0.02 (0.02) |
| 46.67N | 41.25E | 260 | 0.84 | 0.06 (0.06) |

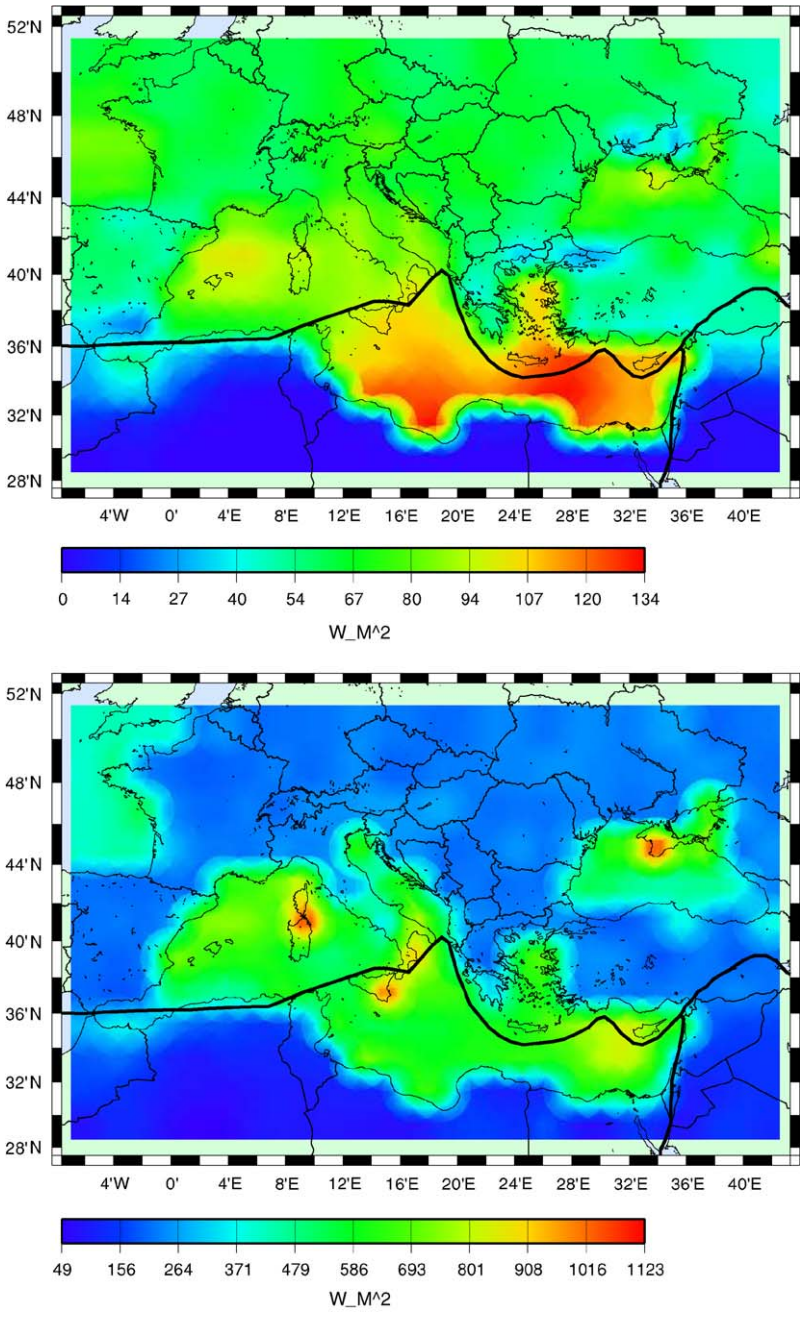


Fig. 2. (Top) Average and (bottom) highest values of SLHF from 1/1/1997 to 31/12/2004.

Fig. 3. This seasonal fluctuation is, nevertheless, more prominent over land than over sea as it is, for instance, over the Italian Alps (grid 244), where the largest difference between winter and summer months is recorded, Turkey (grid 154) and Russia (grid 260). A seasonal pattern is also observed over Morocco (grid 83), although it is now reversed with lows during summer and autumn and highs during winter and spring. Moreover, in Morocco the SLHF fluctuations are smoother during the summer and autumn months. SLHF over the Sahara desert (grid 12) is always very low-almost zero-with scattered sharp peaks of a few $W/m^2$ during winter.

Statistical information on the SLHF time series is provided in Fig. 4 with five boxplot diagrams for various grids, as well as with a diagram presenting averages and standard deviations throughout the year. The

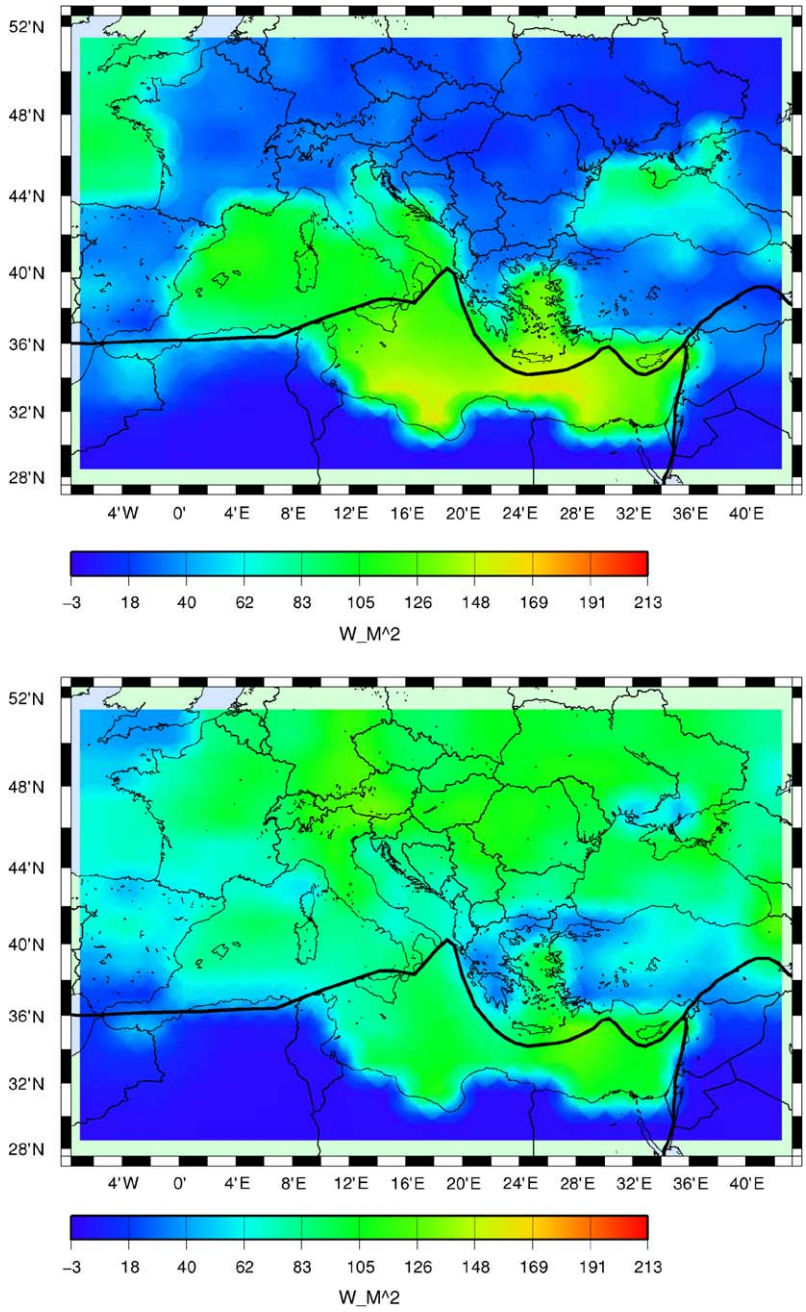


Fig. 3. SLHF average during (top) winter (December to February) and (bottom) summer (June to September) from 1/1/1997 to 31/12/2004.

corresponding SLHF time series are plotted in Fig. 5. The SLHF distributions are asymmetrical exhibiting a positive skew that varies in magnitude per grid. The skewness is less prominent where low SLHF values are observed. It is worth noticing the low variance throughout the year in the desert regions of North Africa (grids 12 and 83). One important information the boxplots can convey, with regard to rare events, is the number of potential ''outliers'', or points that lie above 1.5 times the interquartile range. Such extreme points suggest the presence of strong fluctuations in the SLHF time series, associated with atmospheric phenomena and most importantly with natural hazards.

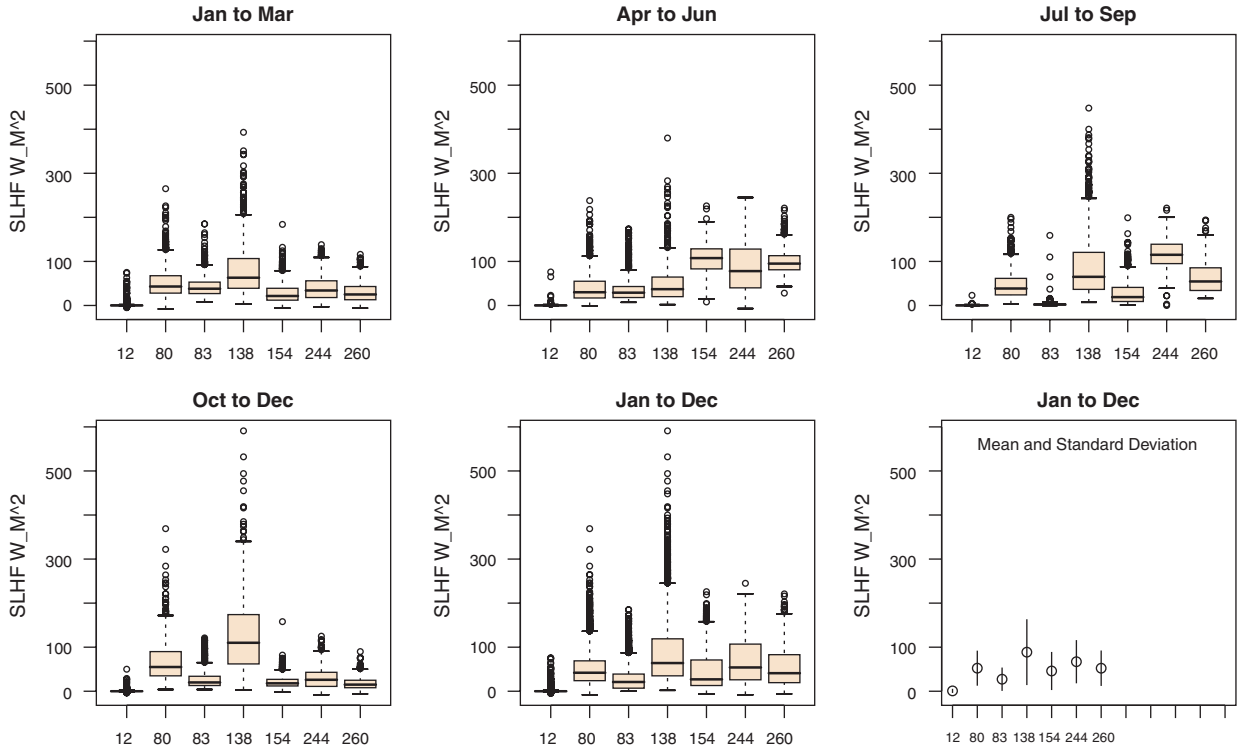


Fig. 4. Statistical distributions of SLHF over selected grids (see Table 1).

### 5.1. Hurst exponent

The nature of long-range correlations within the SLHF records can be explored with the help of the Hurst exponent. A map of the 8-year long global Hurst exponents has been constructed and shown in Fig. 6a. Two distinct regions can be identified: (a) central Europe and (b) sea, the Hurst exponent being in general lower over water than over land. In particular, over sea the SLHF records are uncorrelated or weakly correlated, exhibiting an approximate $H \sim 0.5$ (blue shades). Over Europe, on the other hand, the Hurst exponent suggests the presence of persistent long-range correlations ranging within the interval $[0.5, 1]$ (green, yellow and red shades). Coasts and islands form an intermediate category where the Hurst exponent is weakly persistent. Africa, on the other hand, represents a special case where the long-range correlations span from strong persistence (Algeria) to anti-persistence as in Libya where the smallest value is registered ($H = 0.35$). In contrast, the highest Hurst exponents are registered over Turkey ($H = 0.99$), at the border between Austria and Switzerland ($H = 1.03$) and in Ukraine ($H = 0.93$) (Table 1). The distribution of global Hurst exponents, Fig. 7a, is narrower over the sea and Africa than the rest of land.

To investigate further the origin of the correlations in SLHF records, we shuffle the data[4] of all the time series and reanalyze them. The map of global Hurst exponents after shuffling and their distribution are shown in Figs. 6b and 7b.

The Hurst exponents after shuffling drop to approximately 0.5, indicating not only the removal of correlations but also that these correlations were not a probabilistic attribute of the seasonal variability of SLHF. The seasonal component is, in any case, removed during the normalization process and the DFA. The difference of SLHF patterns between land (persistent correlation) and sea (absence of correlation) suggests the presence of non-periodic elements of SLHF over land, which could be attributed to the long-range

[4]The SLHF time series over each location is shuffled by selecting pairs of values in random and exchanging their positions in time. This procedure is performed twice, expecting that any present correlations would be destroyed.

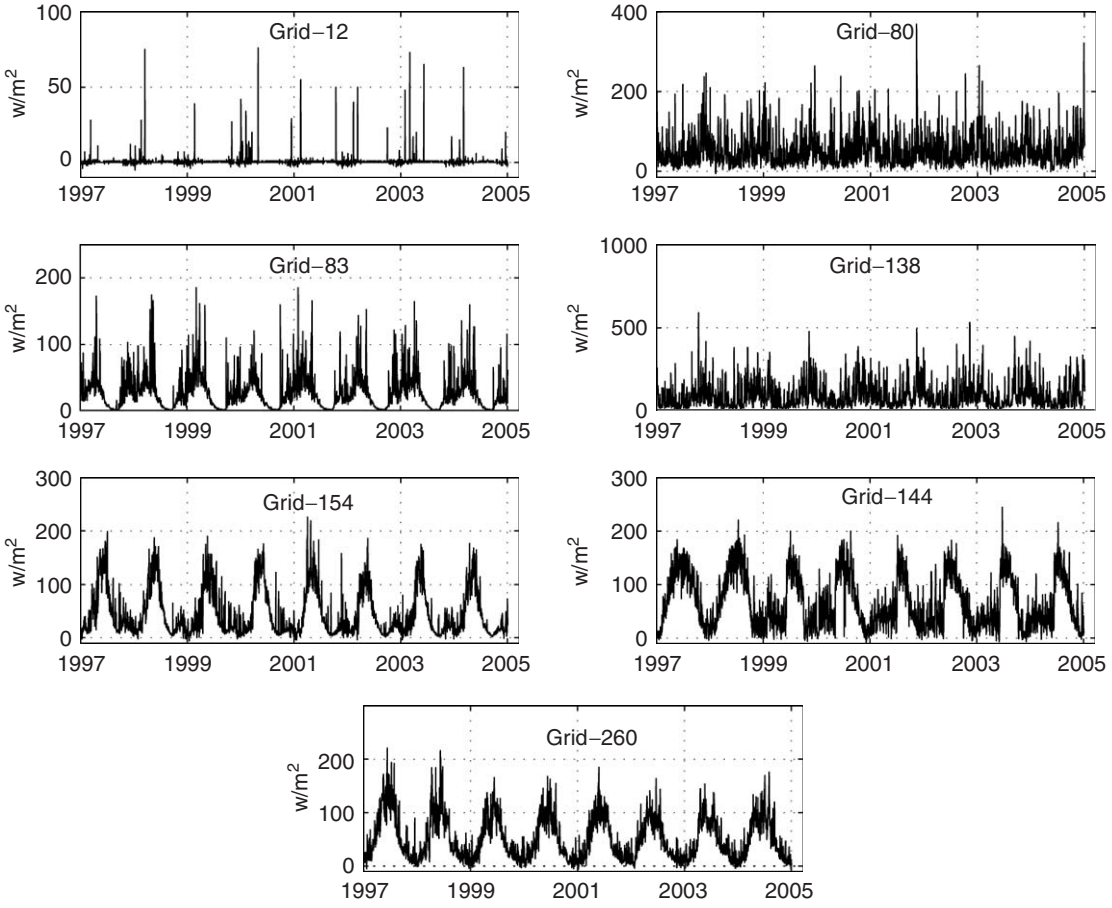


Fig. 5. SLHF time series over selected grids (see Table 1).

correlations observed in rainfall records [35,42,43]. Since SLHF does not have a strong dependence on rainfalls over the sea, the uncorrelated data patterns should be expected. However, the anti-persistence observed over the deserts of Africa, may still be related to the rainfalls in those parts of the world, even though it does not lead to persistent correlations. The reason might be that in the deserts very low SLHF values are generally recorded almost all-year round. For short time periods intense rainfalls take place, which would temporarily yield very high SLHF values and consequently to anti-persistent fractal behavior.

### 5.2. Multifractal analysis

We shall discuss the multifractal character of SLHF at each area on the basis of the range $R$ of the estimated generalized Hurst exponents estimated from the MF-DFA. The range $R$, defined as $R = h(q_{min}) - h(q_{max})$, quantifies the difference between the scaling of small and large fluctuations and can be considered thus as a measure of the heterogeneity of the fractal behavior of SLHF. We begin the discussion with the positive values of parameter $q$ (see Section 4), $R = h(0) - h(5)$, (i.e., the range of middle to large SLHF fluctuations), while the consequences of the negative moments (low SLHF fluctuations and smooth parts of the time series) will be discussed later.

A map of ranges $R$ is shown in Fig. 8 for original and shuffled data while their corresponding distributions are shown in Fig. 9. Africa exhibits stronger multifractal SLHF character, $R = 0.65 \pm 0.18$, in contrast to the majority of the other regions. The highest value of $R$ is observed over east Libya ($R = 0.96$). Among the

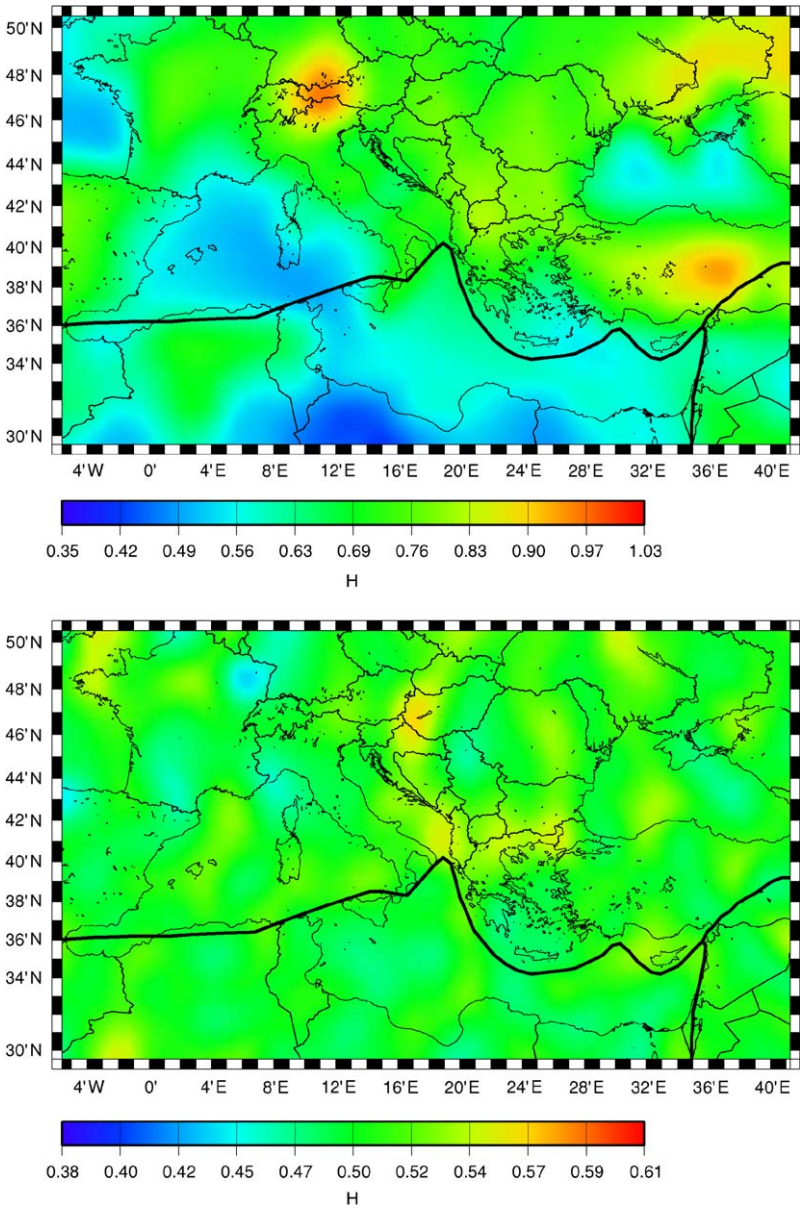


Fig. 6. Map of the global Hurst exponents, $H$, of the (top) normalized original and (bottom) shuffled SLHF time series.

regions of low multifractality the higher $R$ is estimated for the east of Turkey ($R = 0.33$) and Southeast Mediterranean ($R = 0.35$). The lowest $R$ is recorded over South Italy ($R = -0.07$).[5]

The multifractality in the smoother parts of the SLHF time series is investigated by the negative $q$s, as can be explored for $q = -1$. The scaling relation (6) does not now always hold for negative values of $q$ ($-1 < q < 0$). For such negative moments the following cases are observed. Certain regions which exhibit strong multifractality for positive $q$, now exhibit a crossover scale, i.e., two scaling intervals, $N$, each of different scaling exponent, such as in North Africa. On the other hand, for those areas where SLHF was monofractal for positive $q$, relation (6) holds for all $N$ (uniform scaling), such as in North Italy. There are, nevertheless,

[5]Considering that the error in the estimation of $R$ is at the order of 0.1, such negative value is in fact statistically equivalent to zero and indicate monofractal SLHF behavior.

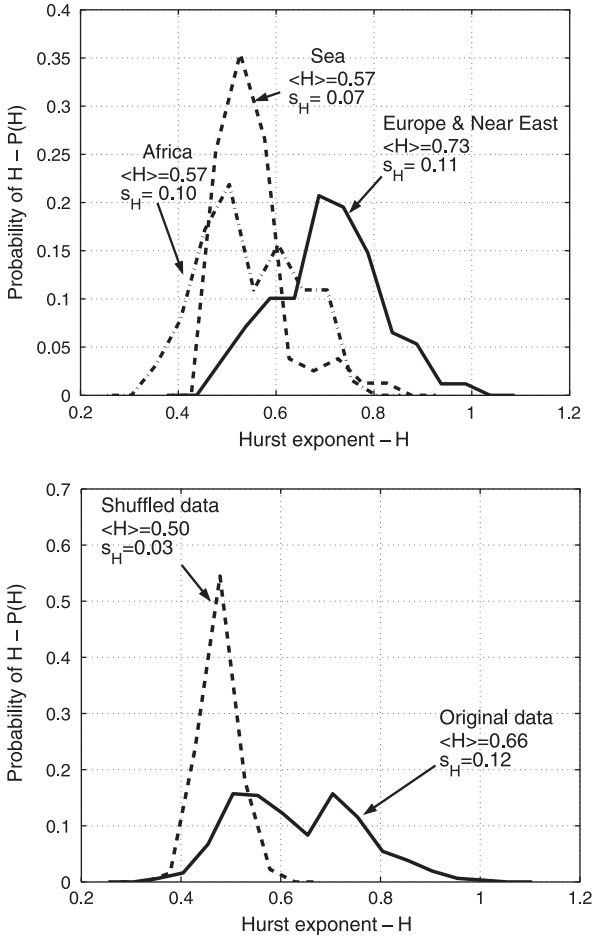


Fig. 7. Distribution of the global Hurst exponents. (Top) Europe and Near East, Africa and sea. (Bottom) Original and shuffled time series.

locations where the scaling collapses completely and the linear relation (6) is no more adequate to describe the behavior of SLHF, such as in Middle East. Characteristic examples of uniform scaling, crossover behavior and collapse of scaling are presented in Fig. 10. The scaling exponents $h(-1)$ for small ($20 < N < 120$) and large values ($120 < N < 500$) of $N$, representing the intensity of short- and long-range correlations are shown in Figs. 11(a) and (b), respectively. Areas for which relation (6) leads to gross errors, indicating the presence of non-linear scaling for small or/and large scales, are colored gray. The observed scales $N$ where crossover occurs range from 40 to 270 days averaging to 120 days. This periodical element in the time series can be attributed to the seasonal component that has survived after the normalization. The long-range correlations in the smooth fluctuations of the SLHF are apparently affected by the seasonal component. However, these periodicities are rather singular than smooth in nature, since they would have otherwise been eliminated by either the DFA or the normalization process.

The scaling of all the moments of the shuffled time series becomes linear regardless of location. This supports the view that the presence of a crossover scale was due to some seasonal element that the shuffling wiped out. The shuffling of SLHF records, Figs. 8b and 9b, decreases their observed multifractality by about 59% on average. This reduction implies that the observed multifractality in Africa was the result of both a broad probability distribution of SLHF records, as well as of a variety in long-range correlation magnitudes for the small and large fluctuations of SLHF. The weak multifractality observed in areas other than Africa can only be attributed to the common origin of the long-range correlations in SLHF in those areas. We have suggested that this is due to the rainfalls.

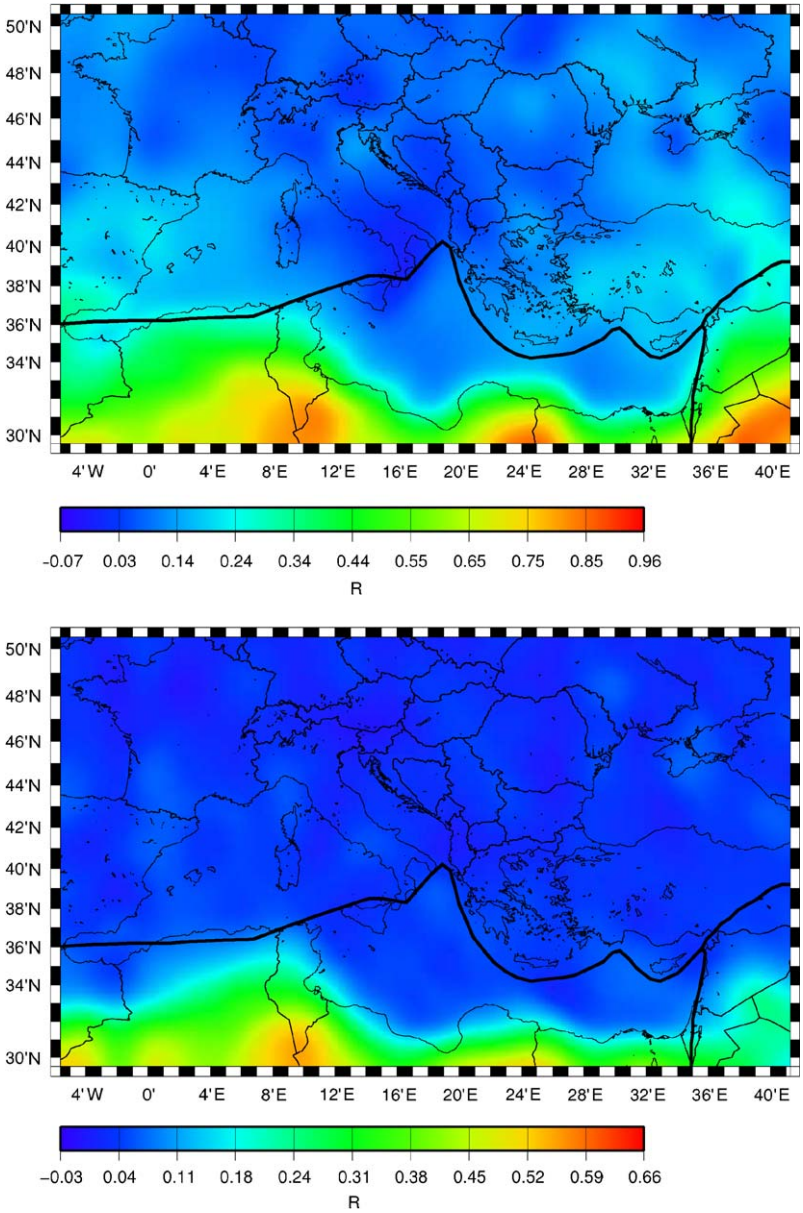


Fig. 8. Map showing the range of generalized Hurst exponents. (Top) $0<q<5$, normalized original SLHF time series. (Bottom) $-1<q<5$, shuffled time series.

## 6. Conclusions

The multifractal analysis of SLHF records over the Mediterranean Sea and the surrounding land, as estimated from data of the last eight years, has led to a quite clear picture regarding this dynamical process. Three distinct regions of similar SLHF multifractal behavior are distinguished: (a) The Mediterranean and Black Seas, (b) Africa and (c) Europe and Near East. An attribute of SLHF is that it is always higher over the sea with a weaker seasonal variability and exhibits monofractality in its time series that indicates uncorrelated data. Over Europe, the seasonal component is much stronger and SLHF shows monofractality and persistence, which is probably related to the long-range correlations induced by rainfalls. The lowest values of SLHF are observed over Africa, where SLHF changes from anti-persistent (deserts) to persistent and presents

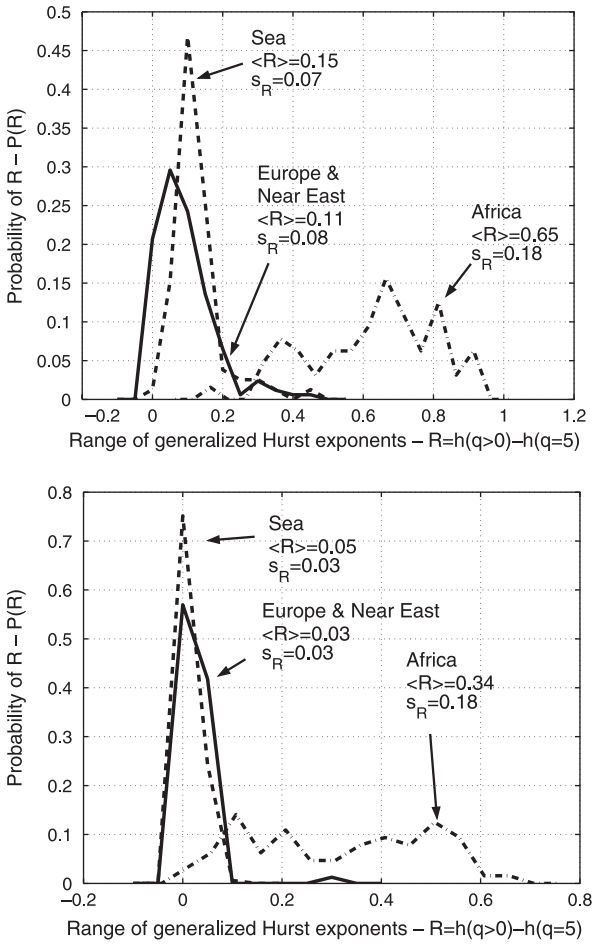


Fig. 9. Distribution of the range of generalized Hurst exponents over Europe and Near East, Africa and sea. (Top) $0<q<5$, normalized original SLHF time series and (bottom) $-1<q<5$, shuffled time series.

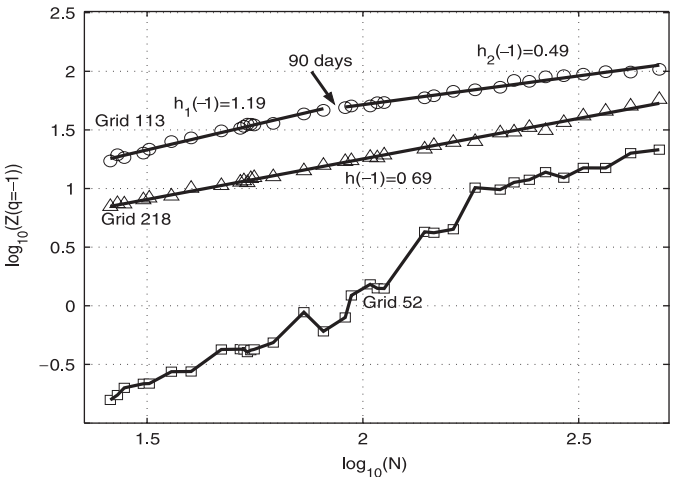


Fig. 10. Scaling of the negative moments for selected grids. Triangles: whole-range linear scaling, grid 218 (North Italy). Circles: crossover of linear scaling at 90 days, grid 113 (North Africa). Squares: non-linear scaling, grid 52 (Middle East).

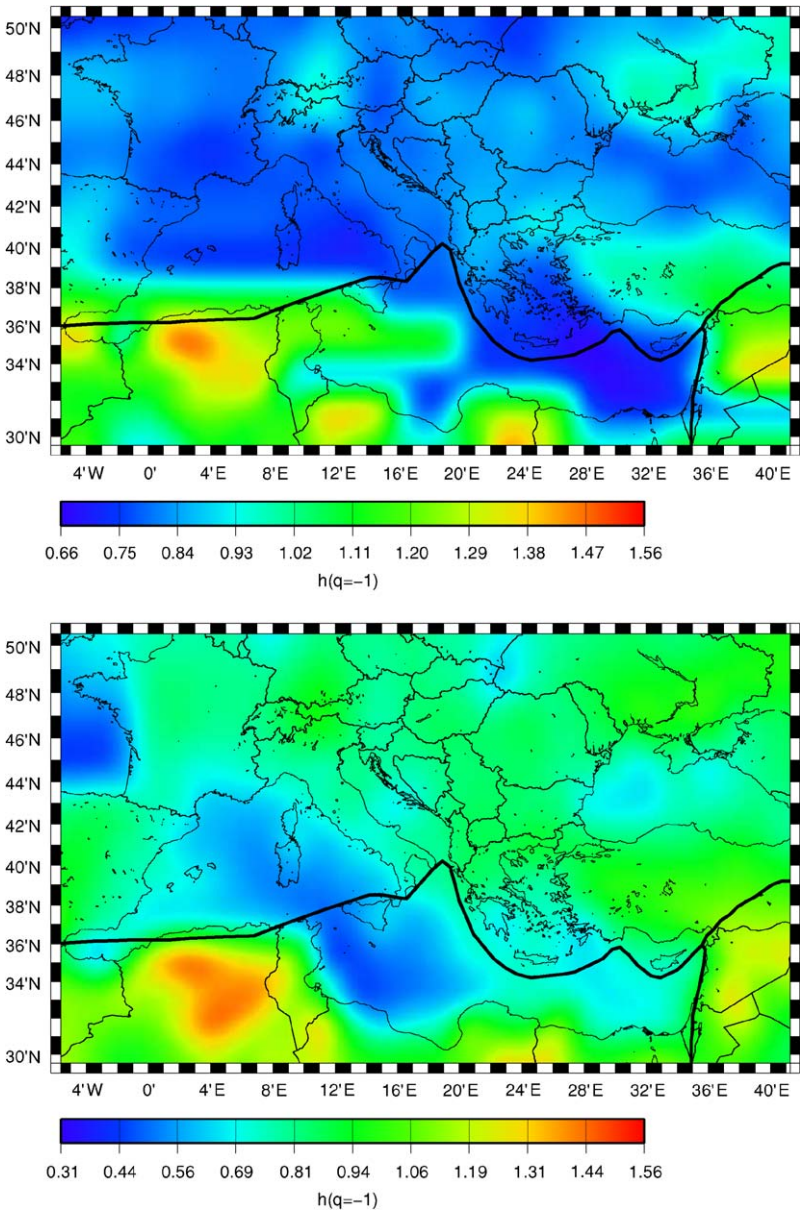


Fig. 11. Generalized Hurst exponent for $q = -1$ over (top) small and (bottom) large scales. Gray areas: regions where linear scaling collapses.

intense multifractality which is due both to a broad probability distribution and a variety of long-range correlations for small and large fluctuations. Moreover, the existence of crossover scales, mainly over the northwest African coasts, implies that the smaller fluctuations of SLHF are affected by seasonal components that survived the normalization.

The application of our results in the field of forecasting and monitoring is straightforward. Possible precursors may be detected related to the appearance of "anomalous" fractal or multifractal characteristics in the short-term behavior of SLHF, as for example significant deviations from the long-term records of the Hurst exponent, or of the range of scaling exponents. Such evaluation by contrast approaches have already been used successfully in the analysis of ULF geomagnetic data [25], where increase of multifractality has been observed prior to large earthquakes and other natural hazards [27,44]. Knowledge of the long-term behavior

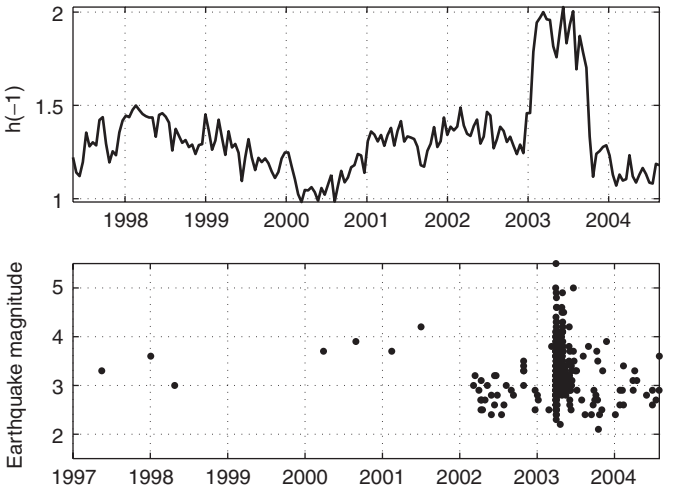


Fig. 12. Generalized Hurst exponent for $q = -1$ and earthquake events over Central Italy (red circle in Fig. 1) during 1997–2004.

of scaling exponents characterizing the SLHF time series over several locations could be, therefore, used as a reference in the short-term prediction analysis. As the box-counting algorithms used in these studies are not applicable on non-stationary data like SLHF, "local" versions of the DFA [45] and the wavelet-based methods [46,47] could be applied instead in order to quantify its fractal behavior over short periods of time.

To this end we have applied the local MF-DFA in the SLHF time series over central Italy, as shown in Fig. 1 (red circle). Taking into account that within the time period of interest strong earthquakes have been rather rare in this region, it is inevitable that we will be studying the effects of almost isolated events on SLHF. We have considered a moving window of 256 days wherein the analysis is performed, according to the discussion in Section 4.2, with the scale parameter $N$ ranging from three weeks to three months. The resulting analysis shows a notable association between the generalized Hurst exponent $h(q = -1)$ and the earthquake events, Fig. 12. During the first six years of the time series, the exponent $h(q = -1)$ remains below 1.5 and rises to almost 2 in the year 2003 when very strong earthquakes have been registered.

The increase of $h(q = -1)$ results from the fact that the smooth parts of the SLHF time series related to it, were even smoother during 2003 than they were in previous years. This could have been brought about by the effect of a deterministic factor, a geophysical process related to strong earthquakes, which advances in time scales from three weeks to three months. Furthermore, since similar multifractal features are observed over most of the neighboring regions, our findings cannot be considered as an artefact of the small window chosen in the analysis and cannot be attributed to errors of evaluation.

This remarkable result is, however, only indicative as a more systematic study is required between the multifractal behavior of SLHF and seismicity in order to draw definite conclusions. As shown in the case presented here, it is very likely that the local SLHF behavior is influenced by the earthquake activity of the neighboring regions. A detailed analysis involving statistical evaluation of related evidence must be performed in order to discriminate between all possible sources of anomalous behavior. The task to test the hypothesis that SLHF multifractality unambiguously correlates with seismicity is reserved for future work.

## Acknowledgments

The Special Account for Research Grants of the University of Athens has financially supported this work.

## References

[1] M. Hayakawa, Y. Fujinawa, Electromagnetic Phenomena Related to Earthquake Prediction, Terra Scientific Company, Tokyo, 1994.

[2] S. Dey, R.P. Singh, Nat. Hazards Earth Syst. Sci. 3 (2003) 749.

[3] G. Cervone, M. Kafatos, D. Napoletani, R.P. Singh, Nat. Hazards Earth Syst. Sci. 4 (2004) 359.
[4] G. Cervone, R.P. Singh, M. Kafatos, C. Yu, Nat. Hazards Earth Syst. Sci. 5 (2005) 87.
[5] B.B. Mandelbrot, The Fractal Geometry of Nature, Freeman, New York, 1983.
[6] J. Feder, Fractals, Plenum Press, New York, London, 1988.
[7] H.-O. Peitgen, H. Jurgens, D. Saupe, Chaos and Fractals: New Frontiers in Science, Springer, New York, 1992.
[8] B.B. Mandelbrot, Multifractals and $1/f$ Noise. Wild Self-Affinity in Physics, Springer, New York, 1998.
[9] U. Frisch, G. Parisi, in: Turbulence and Predictability in Geophysical Fluid Dynamics and Climate Dynamics, North-Holland, Amsterdam, 1985.
[10] B.B. Mandelbrot, Quant. Finance 1 (2001) 641.
[11] D.L. Turcotte, Fractals and Chaos in Geology and Geophysics, Cambridge University Press, Cambridge, 1997.
[12] S. Lovejoy, D. Schertzer, Bull. Am. Meteorol. Soc. 67 (1986) 21.
[13] Y.Y. Kagan, L. Knopoff, Geophys. J. R. Astron. Soc. 62 (1980) 303.
[14] M.B. Geilikman, T.V. Golubeva, V.F. Pisarenko, Earth Planet. Sci. Lett. 99 (1990) 127.
[15] D. Kiyashchenko, N. Smirnova, V. Troyan, F. Vallianatos, Nat. Hazards Earth Syst. Sci. 3 (2003) 285.
[16] M. Sahimi, M.C. Robertson, C.G. Sammis, Phys. Rev. Lett. 70 (1993) 2186.
[17] Y. Ashkenazy, D.R. Baker, H. Gildor, S. Havlin, Geophys. Res. Lett. 30 (2003) 2146.
[18] D. Schertzer, S. Lovejoy, F. Schmitt, Y. Chiguirinskaya, D. Marsan, Fractals 5 (1997) 427.
[19] F. Schmitt, D. Lavallée, D. Schertzer, S. Lovejoy, Phys. Rev. Lett. 68 (1992) 305.
[20] P.A. Varotsos, N.V. Sarlis, E.S. Skordas, Phys. Rev. E 66 (2002) 011902.
[21] P.A. Varotsos, N.V. Sarlis, E.S. Skordas, Phys. Rev. E 67 (2003) 021109.
[22] N. Scafetta, B.J. West, Phys. Rev. Lett. 92 (2004) 138501.
[23] P.G. Kapiris, K.A. Eftaxias, T.L. Chelidze, Phys. Rev. Lett. 92 (2004) 065702.
[24] S. Nakaya, T. Hashimoto, Geophys. Res. Lett. 29 (2002) 133.
[25] Y. Ida, M. Hayakawa, A. Adalev, K. Gotoh, Nonlinear Process. Geophys. 12 (2005) 157.
[26] Y.S. Baryshnikova, G.M. Zaslavsky, E.A. Lupyan, S.S. Moiseyev, E.A. Sharkov, Adv. Space Res. 9 (1989) 405.
[27] P.P. Dimitriu, E.M. Scordilis, V.G. Karacostas, Nat. Hazards 21 (2000) 277.
[28] S. Chou, E. Nelkin, J. Ardizzone, R.M. Atlas, J. Climate 17 (2004) 3973.
[29] M. Pidwirny, ⟨http://www.physicalgeography.net/⟩, (2004).
[30] R.B. Stull, An Introduction to Boundary Layer Meteorology, Kluwer Academic Publishers, Dordrecht, 1988.
[31] A. Bentamy, K.B. Katsaros, A.M. Mestas-Nuez, W.M. Drennan, E.B. Forde, H. Roque, J. Climate 16 (2003) 637.
[32] R. Gautam, G. Cervone, R.P. Singh, M. Kafatos, Geophys. Res. Lett. 32 (2004) L04801.
[33] Y. Sadhuram, B.P. Rao, D.P. Rao, P.N.M. Shastri, M.V. Subrahmanyam, Nat. Hazards 32 (2004) 191.
[34] E. Kalnay, M. Kanamitsu, R. Kistler, W. Collins, D. Deaven, L. Gandin, M. Iredell, S. Saha, G. White, J. Woollen, Y. Zhu, M. Chelliah, W. Ebisuzaki, W. Higgins, J. Janowiak, K.C. Mo, C. Ropelewski, J. Wang, A. Leetmaa, B. Reynolds, R. Jenne, D. Joseph, Bull. Am. Meteorol. Soc. 77 (1996) 437.
[35] H.E. Hurst, Trans. Am. Soc. Civ. Eng. 116 (1951) 770.
[36] B.B. Mandelbrot, J.W. Van Ness, SIAM Rev. 10 (1968) 422.
[37] F. Pallikari, Chaos Soliton Fract. 12 (2001) 1499.
[38] T. Karagiannis, M. Faloutsos, R. Riedi, IEEE GLOBECOM, Global Internet Symposium, 2002.
[39] J.F. Muzy, E. Bacry, A. Arneodo, Phys. Rev. Lett. 67 (1991) 3515.
[40] J.W. Kantelhardt, S.A. Zschiegner, E. Koscielny-Bunde, A. Bunde, S. Havlin, E.H. Stanley, Physica A 316 (2002) 87.
[41] N. Papasimakis, Diploma Thesis, University of Athens, 2005.
[42] H.E. Hurst, Nature 180 (1957) 494.
[43] O. Peters, C. Hertlein, K. Christensen, Phys. Rev. Lett. 88 (2002) 018701.
[44] A. Ramirez-Rojas, A. Munoz-Diosdado, C.G. Pavia-Miller, F. Angulo-Brown, Nat. Hazards. Earth Sys. Sci. 4 (2004) 703.
[45] Z.R. Struzik, Local scaling analysis with continuous DFA method, CWI report, 2003, unpublished.
[46] Z.R. Struzik, Fractals 8 (2000) 163.
[47] P. Goncalves, P. Abry, ICASSP, vol. 5, 1997, p. 3433.